3D aeromagnetic imaging of Iwate volcano, northeast Japan

Shigeo Okuma*
Geological Survey of Japan, AIST
AIST Tsukuba Central 7,
Higashi 1-1-1, Tsukuba,
305-8567 Japan
s.okuma@aist.go.jp

Tadashi Nakatsuka
Geological Survey of Japan, AIST
AIST Tsukuba Central 7,
Higashi 1-1-1, Tsukuba,
305-8567 Japan
tad.nktk@nifty.com

Ryota Kageura
Nippon Engineering Consultants Co., Ltd
Shintoshin 11-2, Chuo-ku, Saitama
330-6011 Japan
kageura@ne-con.co.jp

SUMMARY

Iwate volcano, northeast Japan is an active Quaternary volcano and is comprised of two parts: West-Iwate and East-Iwate. These bodies are underlain by early–middle Pleistocene volcanic rocks. In 1999, fumarolic areas were newly emerged along the ridge between Ubakura and Kurokura Mountains in West-Iwate and Iwate volcano was thought that an eruption was impending in 2000. However, the fumarolic activity has decreased since its peak in July 2001, and the disaster seems to have passed.

In late 2000, a helicopter-borne EM and magnetic survey was conducted over Iwate volcano to better understand the subsurface structure of the volcano related to the ongoing volcanic activity. Recently we have conducted three-dimensional (3D) imaging of Iwate volcano to constrain its subsurface structure. Our model indicates that magnetization highs occupy the main edifice of East-Iwate, which reflects the surface and/or subsurface distribution of basaltic lavas. Meanwhile, magnetization lows are dominant inside the summit caldera of West-Iwate except for a magnetic high over the Onashiro lava flow. Magnetization highs are also distributed on the northern and southern slopes of West-Iwate but local magnetization lows lie on the heads of narrow valleys, corresponding to hydrothermal altered areas. These hydrothermal altered areas are also characterized by resistivity lows observed by the Airborne EM survey.

Although the imaging improved our understanding of the surface and subsurface distribution of volcanic rocks in Iwate volcano, some limitations exist. No information about the magmas which should have intruded during the recent eruptive crisis was obtained by the imaging. The small magnetic contrast between the intruded magmas and their host rocks is the most probable reason.

Key words: Iwate volcano, 3D imaging, magnetization, aeromagnetic anomalies, helicopter-borne EM and magnetic survey

INTRODUCTION

Iwate volcano, northeast Japan is an active Quaternary volcano and divided into two parts: West-Iwate and East-Iwate (Figure 1). West-Iwate volcano has a 2.5 km long by 1.5 km wide caldera on the summit, whereas East-Iwate volcano is a basaltic stratocone. These bodies are underlain by early - middle Pleistocene volcanic rocks such as Matsukawa andesites and Amihari Volcanic Group (Itoh and Doi, 2005).

Since volcanic tremors had been observed 8 km below East- Iwate in 1995, the seismicity increased with the crustal deformation of West-Iwate.

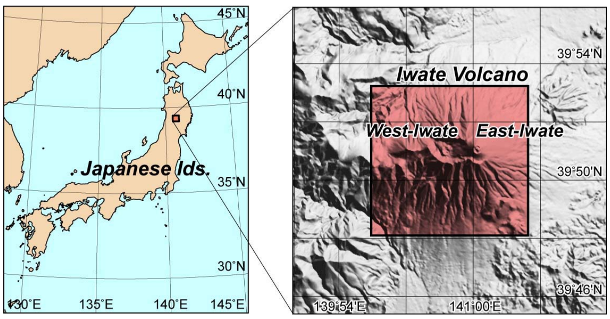

Figure 1 Location map of study area (after Okuma et al., 2008). The red rectangle of the right panel indicates the study area.

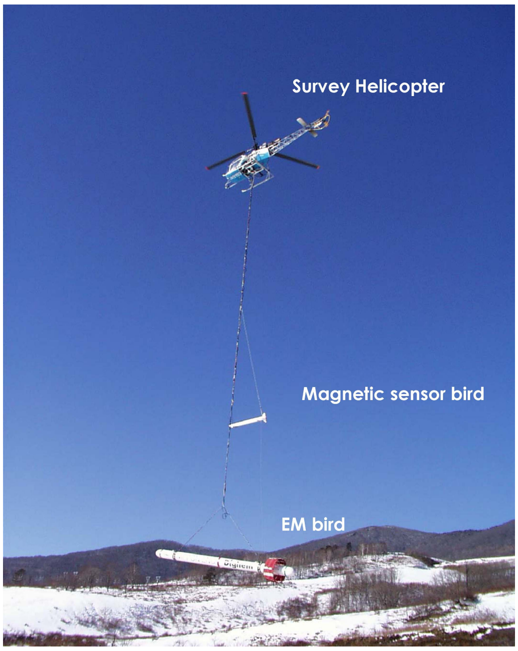

Photo 1 Picture of the survey helicopter (SA315B) used for the airborne EM and magnetic survey over Iwate volcano (Okuma et al., 2008). Birds for magnetics and EM were suspended from the helicopter

In 1999, fumarolic areas were newly emerged along the ridge between Ubakura and Kurokura Mountains in West-Iwate and Iwate volcano was thought that an eruption was impending in 2000. However, the fumarolic activity has decreased since its peak in July 2001, and the disaster seems to have passed.

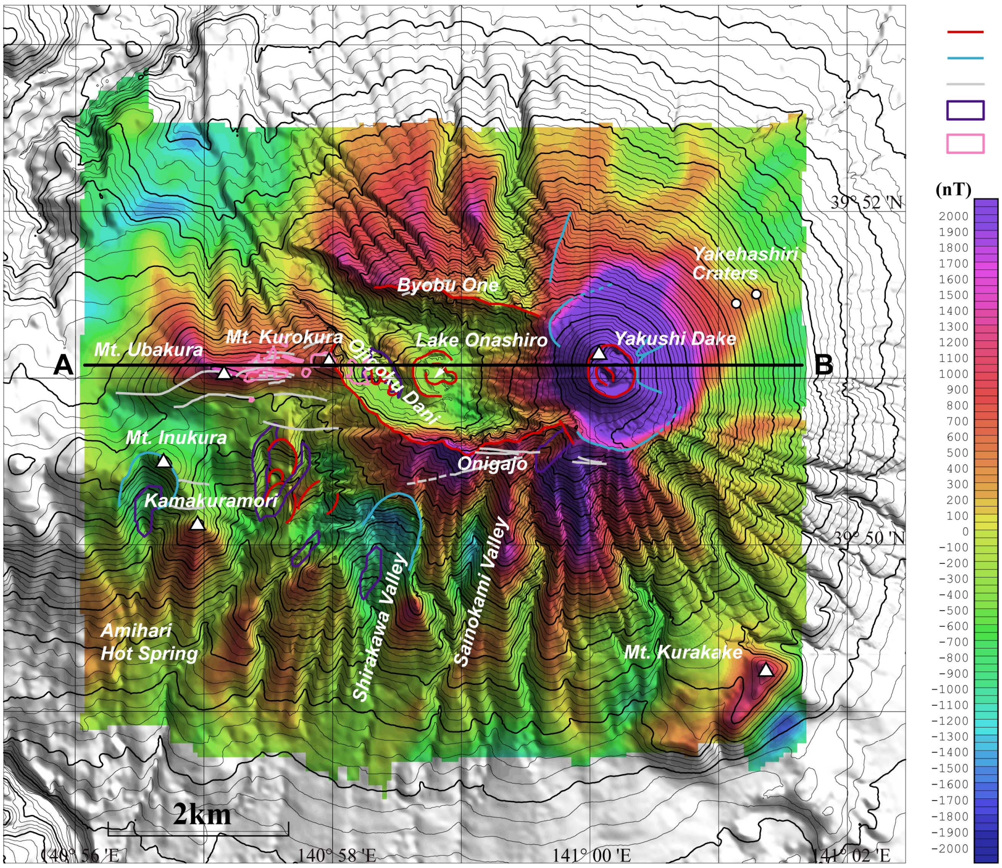

Figure 2 Reduction to the pole anomalies with topographic shading and contours (modified from Okuma et al., 2008). Profile A-B shows the location of apparent resistivity and magnetization cross-sections (Figure 4). Magnetic contour interval is 100 nT.

AIRBORNE EM AND MAGNETIC SURVEY

From November to December 2000, a helicopter-borne EM (HEM) and magnetic survey was conducted over Iwate volcano (Figure 1) to better understand the subsurface structure of the volcano related to the ongoing volcanic activity and to evaluate the slope stability of the volcano (Okuma et al., 2008). The HEM system is a modified DIGHEM-V model that is operated at five frequencies from 220 Hz to 137,500 Hz with five-fold frequency increments. The survey was flown using an SA315B (Lama; Photo 1) at an altitude of 70 m above the terrain along north-south survey lines and east-west tie lines, spaced 100 m and 1,000 m apart, respectively. A magnetic sensor bird and an EM bird were towed 25 m and 35 m below the helicopter, respectively. The observed electromagnetic data were processed and apparent resistivity maps were created for each five frequencies. Cross-sections of apparent resistivity profiles were also calculated from an interpolation of apparent resistivity data at five frequencies. Whereas, the observed magnetic data were processed and total magnetic intensity anomalies were compiled on a smoothed observed surface (Okuma et al., 2008), assuming equivalent anomalies below observation surface (Nakatsuka and Okuma, 2006). The reduction to the pole anomalies (Figure 2) were also calculated from the total magnetic intensity anomalies on the surface.

The magnetic survey revealed the subsurface extension of volcanic rocks, especially basaltic - andesite lavas and weakly magnetized areas probably demagnetized by alteration.

According to the reduction to the pole anomaly map (Figure 2), the characteristics of the magnetic anomalies over the volcano are summarized as follows (Okuma et al., 2008):

(1) In East-Iwate, apparent magnetic highs lie on the Yakushi Dake stratocone and its basaltic lava flows. Magnetic highs are also distributed on the north and south ridges of East-Iwate. Magnetic highs are aligned linearly to the northeast at the Yakehashiri Nos.1 and 2 craters which produced basaltic lavas in 1732 (Itoh and Doi, 2005).

(2) In West-Iwate, magnetic highs lie over the main edifice composed mainly of andesitic volcanic rocks. Magnetic lows are dominant inside the summit caldera except for a magnetic high over the Onashiro lava flow.

(3) Apparent magnetic lows are observed over some areas of the Amihari Volcanic Group (Itoh and Doi, 2005) south of Mt. Inukura and Shirakawa valley, corresponding obviously to hydrothermally altered zones. This result suggests the upper stream of the Sainokami valley is also underlain by a hydrothermal altered zone. No obvious features were found at the newly emerged fumarolic areas along the ridge between Ubakura and Kurokura Mountains, implying the demagnetization of the volcanic rocks, which compose the areas, was not so strong.

3D IMAGING AND RESULT

Using a vector/matrix notation, the magnetic anomaly $\boldsymbol{f}$ at an observation point is expressed as follows:

$$\boldsymbol{f} = \boldsymbol{As} \tag{1}$$

where $\boldsymbol{f}$ is the magnetic anomaly, $\boldsymbol{A}$ is a geometric factor, and $\boldsymbol{s}$ is magnetization of the source.

We adopted the 3D imaging method proposed by Nakatsuka and Okuma (2014) to solve the equation (1). In order to regularize a simple CG method, a penalty term is added in the minimizing function as:

$$(\boldsymbol{f} - \boldsymbol{As})^{\mathrm{T}} (\boldsymbol{f} - \boldsymbol{As}) + e\,(\boldsymbol{Bs})^{\mathrm{T}} (\boldsymbol{Bs}) \rightarrow \mathrm{Min} \tag{2}$$

where $\boldsymbol{B}$ is the penalizing operator matrix, and e is a trade-off parameter (so-called hyper-parameter) to adjust the penalizing weight ratio between the former misfit term $(\boldsymbol{f} - \boldsymbol{As})^{\mathrm{T}} (\boldsymbol{f} - \boldsymbol{As})$ and the latter regularization term $R=(\boldsymbol{Bs})^{\mathrm{T}} (\boldsymbol{Bs})$ in (2).

In the case of a model composed of variable volume bodies, the penalizing operator and the regularizing factor should be

$$\boldsymbol{B} = \mathrm{diag}\left\{ \sqrt{\frac{v_i}{s_i^2 + \delta^2}} \right\} \tag{3}$$

$$R = (\boldsymbol{Bs})^{\mathrm{T}} (\boldsymbol{Bs}) = \sum_i \frac{v_i s_i^2}{s_i^2 + \delta^2} \tag{4}$$

where v_i is volume of the i-th body, and δ is critical value of magnetization.

To better estimate the detailed structure of the volcano, we applied 3D magnetic imaging to the observed total magnetic intensity anomalies (Okuma et al., 2008), allowing 3D variations of the magnetization intensity. The magnetic model with a flat bottom is composed of magnetic layers with a constant thicknesses varying from 250 m to 1,000 m, except the uppermost one, and each layer consists of an ensemble of prism models with a horizontal dimension of 100 m by 100 m. The bottom depth of the magnetic structure was assumed to be 5 km below the sea level.

The iterative procedure of the imaging method was started using a uniform magnetization of 4.3 A/m as the initial starting value, which was derived from the average terrain magnetization. δ was 1.0A/m. It was terminated when the rms of residuals of the observed and calculated field were 15.9 nT. Figures 3 and 4 show depth slices and E-W cross sections, respectively, from the imaging, respectively. Additional information such as apparent resistivities (Okuma, 2005) were superimposed on Figure 4.

Figures 3 and 4 indicate that magnetization highs occupy the main edifice of East-Iwate, which reflects the surface and/or subsurface distribution of basaltic lavas. Meanwhile, magnetization lows are dominant inside the summit caldera of West-Iwate except for a magnetic high over the Onashiro lava flow. Magnetization highs are also distributed on the northern and southern slopes of West-Iwate but local magnetization lows lie on the heads of narrow valleys, corresponding to hydrothermal altered areas. These hydrothermal altered areas are also characterized by resistivity lows observed by the Airborne EM survey (Okuma, 2005).

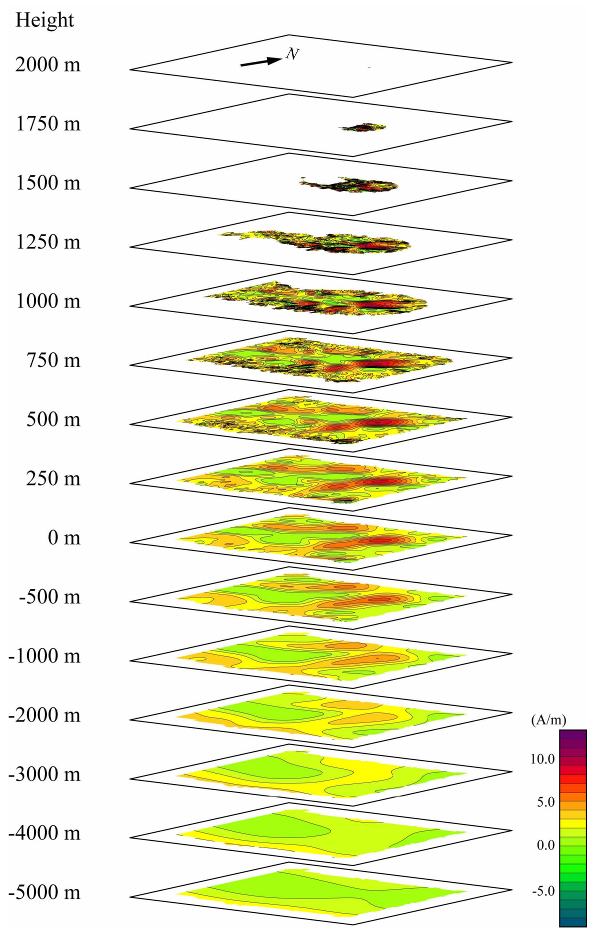

Figure 3 Depth slices of the result of 3D magnetic imaging of Iwate volcano. The depths in the map represent the bottom depths of each layer. The magnetic model with a flat bottom is composed of 15 magnetic layers with a constant thickness from 250 m to 1,000 m for all layers except the uppermost one, and each layer consists of an ensemble of prism models with a horizontal dimension of 100 m by 100 m.

Relative magnetization lows are imaged in the shallow parts of the ridge between Ubakura and Kurokura Mountains and might correspond to the newly emerged fumarolic areas (Figures 2 and 4).

Although the imaging improved our understanding of the surface and subsurface distribution of volcanic rocks in the edifice and basement of Iwate volcano, and further the demagnetization effect probably by the intense fumarolic activity, some limitations exist. No information about the magmas which should have intruded during the recent eruptive crisis was obtained by the survey. The small magnetic contrast between the intruded magmas and their host rocks is the most probable reason. Perhaps the intruded magmas had not cooled enough to become strongly magnetized by the time the survey was conducted.

This relationship implies a similarity between the high-resolution aeromagnetic survey of Usu volcano, Hokkaido, Japan conducted right after its 2000 eruption and the result of 3D aeromagnetic imaging of the volcano (Okuma, et al., 2014).

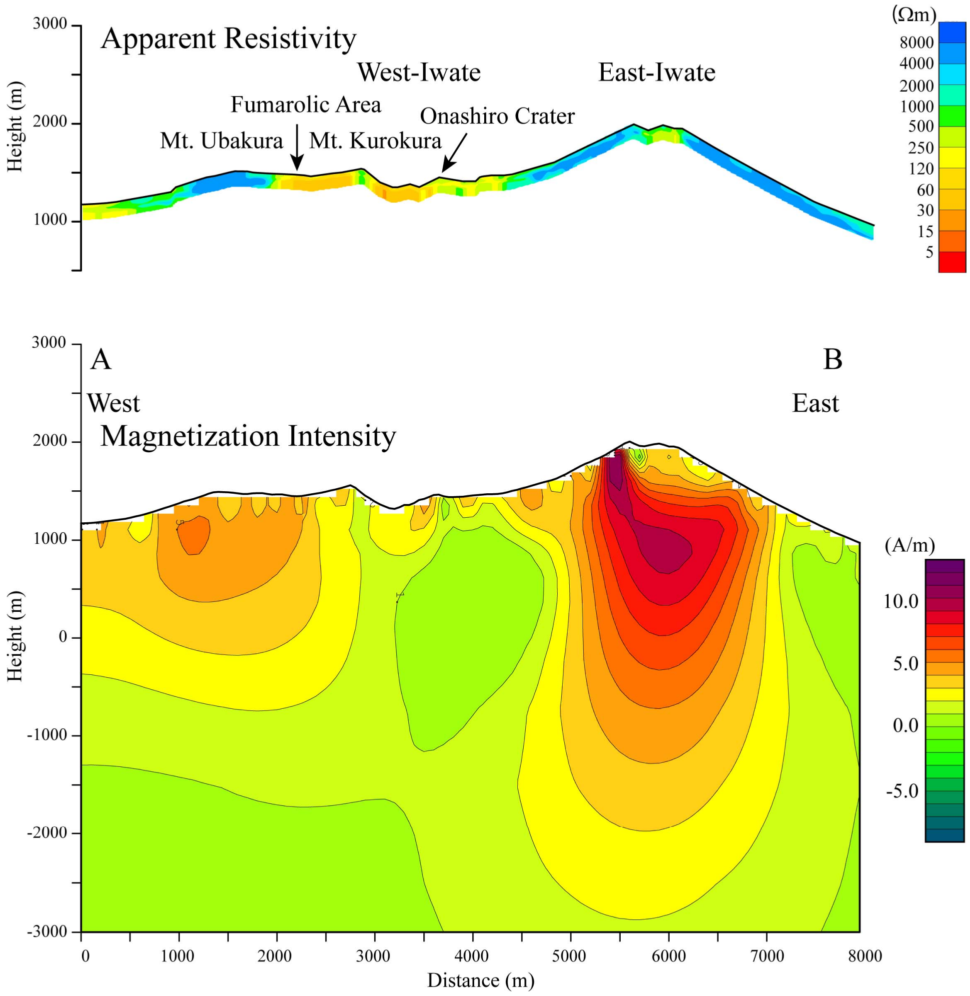

Figure 4 Cross-section of the profile A-B on Figure 2. Upper and lower panels show the apparent resistivity (Okuma, 2005) and magnetization intensity (this study) sections, respectively. The parts deeper than 3km BSL were omitted for convenience.

CONCLUSIONS

We have conducted 3D aeromagnetic imaging of Iwate volcano to better understand its subsurface structure.

The imaging improved our understanding of the distribution of volcanic rocks of Iwate volcano, and furthermore the demagnetization effect probably by the intense fumarolic activity but some limitations exist. Information about the magmas which should have intruded during the recent eruptive crisis was not obtained by the survey. Perhaps the intruded magmas had not cooled enough to become strongly magnetized by the time the survey was conducted.

Consequently, it is not easy to get useful information associated with volcanic activity from a single survey. In this case, repeat aeromagnetic survey might be helpful to extract temporal magnetic anomaly changes over active volcanoes.

REFERENCES

Itoh, J. and Doi, N., 2005, Geological Map of Iwate Volcano, *Geological Map of Volcanoes*, **13**, Geological Survey of Japan, AIST.

Nakatsuka, T., and Okuma, S., 2006, Reduction of geomagnetic anomaly observations from helicopter surveys at varying elevations. *Exploration Geophysics*, **37**, 121-128. DOI: 10.1071/EG06121

Nakatsuka, T., and Okuma, S., 2014, Aeromagnetic 3D subsurface imaging with effective source volume minimization and its application to data from the Otoge cauldron, Shitara, Central Japan. *Exploration Geophysics*, **45**, 16-23. DOI: 10.1071/EG13022

Okuma, S., 2005, Airborne EM and Magnetic Survey. Records of measures against the Iwate volcanic crisis in 1988 supervised by Saito, T., 196-198, Iwate Office of River and National Highway, Tohoku Regional Bureau, MLIT and Iwate Pref. (in Japanese).

Okuma, S., Nakatsuka, T., Morijiri, R. and Takakura, S., 2008, High-reolustion Aeromagnetic Anomaly Map of Iwate Volcano, *Total Intesnity Aeromagnetic Maps*, **44**, Geological Survey of Japan, AIST.

Okuma, S., Nakatsuka, T. and Ishizuka, Y., 2014, Aeromagnetic Constraints on the Subsurface Structure of Usu Volcano, Hokkaido Japan. *Exploration Geophysics*, **45**, 24-36. DOI: 10.1071/EG13041